Received: 10 March 2020 | Revised: 21 March 2021 | Accepted: 6 April 2021

DOI: 10.1002/ldr.3969

RESEARCH ARTICLE

WILEY

Analysis and prediction of land cover changes using the land change modeler (LCM) in a semiarid river basin, Iran

Sajad Khoshnood Motlagh[1] | Amir Sadoddin[1] | Amin Haghnegahdar[2] | Saman Razavi[2] | Abdolrassoul Salmanmahiny[3] | Khalil Ghorbani[4]

[1]Department of Watershed Management, Gorgan University of Agricultural Sciences and Natural Resources, Gorgan, Iran

[2]Global Institute for Water Security, University of Saskatchewan, Saskatoon, Canada

[3]Department of Environment, Gorgan University of Agricultural Sciences and Natural Resources, Gorgan, Iran

[4]Department of Water Engineering, Gorgan University of Agricultural Sciences and Natural Resources, Gorgan, Iran

Correspondence
Amir Sadoddin, Department of Watershed Management, Gorgan University of Agricultural Sciences and Natural Resources, Gorgan, Iran.
Email: amir.sadoddin@gau.ac.ir; amir.sadoddin@gmail.com

Funding information
Global Institute for Water Security, University of Saskatchewan; University of Saskatchewan; Gorgan University of Agricultural Sciences and Natural Resources

Abstract

Predicting future land cover (LC) changes is an important step in the proper planning and management of watersheds. As a susceptible area to salinity and desertification, receiving only about 195 mm rainfall annually, the Hable-Rud River basin is especially sensitive to land use/cover changes. Based on corrected LANDSAT satellite images for the years 1986, 2000, and 2017, the LC were extracted using the maximum likelihood (ML) method. LC changes were predicted by applying the land change modeler (LCM) for the basin. The kappa index for classification in 1986, 2000, and 2017 was 75, 78, and 81%, respectively. Using LCM, the prediction was accomplished for the year 2017 with a kappa index of above 74%. The LC map was predicted for year 2040. The analysis indicates that over the past 32 years, bare land, saline land, agricultural, industrial, and residential areas have increased by about 8, 6.2, 2.7, 0.63, and 0.48%, respectively; while rangeland area was decreased by 18%. Results also indicate that given the predicted LC for year 2040 in comparison with the reference year (2017), saline land, agricultural, industrial, and residential areas will be likely to continue to increase by about 3, 1.5, 0.7, and 0.8%, respectively, whereas bare land and rangeland will most likely decrease by about 4.55 and 1.45%, respectively. The findings of this study assist in analyzing the future trends of LC changes in the basin. This information can be used as a guide for land planners and managers in future land use planning of the area.

KEYWORDS
Hable-Rud River basin, land change modeler, land change prediction, remote sensing, semiarid river basin

1 | INTRODUCTION

The dynamic and sometimes substantial transformation in land use/land cover (LULC) occurs due to socio-economic and natural changes. Although reasons for land cover changes vary depending on the nature and extent of the area, the main drivers can be identified as deforestation, rangeland degradation, and expansion of agriculture (Bezak et al., 2015). Such changes may lead to unfavourable effects on vulnerable ecosystems (Magesh & Chandrasekar, 2017) and are important indicators in understanding the interactions between human activities and environmental functions (Dewan et al., 2012). According to Turner & Moss (1993), land-cover refers to the biophysical attributes of the earth's surface and immediate subsurface. It includes four variables such as land, water, air, and human activity. Land-use is a description of how people utilize the land for their needs by various management practices (Fisher et al., 2005; IPCC, 2000). The LULC pattern of a region is an outcome of natural and socio-economic factors and their utilization by humans in time and space (Moss, 1987). Land use change generally results in the conversion of a piece of land and depicts how it is used and managed (Verburg et al., 2011).

Analysis and prediction of LULC changes allows us to assess ecosystem changes and their environmental consequences at various temporal and spatial scales (Di Gregorio & Jansen, 2000; Lambin, 1997). It is possible to build a model to predict the trends in land cover (LC) changes in a certain period using classified maps of the past. Such information could provide a basis for scientific and effective land-cover planning, management, and ecological restoration and guides regional socio-economic development. Commonly used models for estimating LULC changes are analytical equation-based models (Usharani & Lakshmanaperumalsamy, 2011), statistical models (Paegelow & Camacho Olmedo, 2005), evolutionary models (Aitkenhead & Aalders, 2009), cellular automata models (Farjad et al., 2017; Singh et al., 2015), Markov models (Yang et al., 2012), the SLEUTH model (Mahiny & Clarke, 2012), hybrid models (Subedi et al., 2013), expert system models (Stefanov et al., 2002), and multigene models (Ralha et al., 2013). Various techniques of LULC change detection analysis were discussed by Lu et al. (2004). Traditionally, the method of monitoring LULC changes consisted of field studies combined with large-scale aerial photography, which is often time-intense, meticulous, and costly (Groom et al., 2006).

Over the past few decades, the application of remote sensing technology and geographical information systems (GIS) has gained momentum in landscape dynamics assessment in regional as well as global scales (Atzberger, 2013; Bhat et al., 2017). Satellite imagery is used for the recognition of synoptic data of the earth's surface (Ulbricht & Heckendorff, 1998) and in this context, thematic mapper (TM) and enhanced thematic mapper plus (EMT+) data of LANDSAT have been widely used in studies of LULC since 1972, the start year of the LANDSAT programme (Zheng et al., 2015). Researchers have made extensive attempts to develop advanced classification methods and techniques to improve classification accuracy, including: cellular automata (CA), artificial neural network (ANN), fuzzy logic (FL), intelligent systems (IS), and tree decision (TD) (Lu et al., 2004). Among these, CA is an object-based algorithm increasingly used to simulate the dynamics of natural and human systems and to predict their evolution (Marceau et al., 2013). Despite its simplicity, it can exhibit remarkably rich behavior and is efficient in extracting realistic simulations of land use classes and other spatial structures (Marceau et al., 2013). This algorithm has been widely used in previous studies to identify LC classes (see Etemadi et al., 2018; Feng et al., 2012; Ghorbani Kalkhajeh & Jamali, 2019; Islam et al., 2018; Ozturk, 2015). These studies have shown that CA models are efficient in producing practical simulations of land cover patterns and other spatial structures. CA algorithm is an extension of the land change modeller (LCM) to help predict LC changes using the descriptive variables such as elevation, slope, aspect, and distance from specific areas (Gu et al., 2019; Peraza-Castro et al., 2018; Sangermano et al., 2012).

Land cover changes in arid and semiarid regions can lead to the rapid expansion of desert areas. The Hable-Rud River basin (HRB) has recently encountered desertification problems in its' south. It receives very low precipitation in some parts of the basin (95 mm), and has a large area of saline lands (1,800 km^2) in the southern parts of the basin due to the presence of evaporative sediments. Thus, the changes in land cover in this region can affect both the quantity and quality of water, as well as wind and water erosion severity in the HRB. Therefore, HRB requires assessment of LC changes for better management, planning, and policy-making. Thus, the main objective of this study was to quantify LC changes over the last 32 years (1986–2017) and predict them for the year 2040 using LANDSAT enhanced thematic mapper (ETM) and LANDSAT thematic mapper (TM) images. Hence, this research attempts to answer the following questions: (a) what are the major LC changes in the HRB? (b) what are the main trends of LC changes for the past and the future in the basin? and (c) what are the likely environmental consequences of the LC changes in the HRB? To this end, the CA and maximum likelihood classifier algorithms were used. Since no such work has been conducted in the area before, the outcomes of this study can support decisions on water scarcity and potential risks in the study area.

2 | MATERIALS AND METHODS

2.1 | Study area

The HRB, with an area of about 12,700 km^2, is located between 34° 26′ 54″ to 35° 57′ 31″ N latitudes and 51° 39′ 52″ to 53° 8′ 46″ E longitudes. This basin straddles the border between the Tehran and Semnan provinces in Iran. Situated within the basin are the cities of Firouzkouh and part of Damavand in Tehran Province, and Garmsar, Sorkh, Aradan, and Eyvanekey in Semnan Province. The geographic location of HRB is shown in Figure 1. Due to differences in environmental and natural characteristics, the basin is divided into northern and southern regions. Most of the northern region is mountainous, while a large part of the southern region is in the plains. Average annual precipitation and temperature in the northern part are about 400 mm and 11°C, respectively, while in the southern part these are about 125 mm and 18°C, respectively. Evapotranspiration (ET) is high and the average potential ET can reach to 1,500 mm yr^{-1} in the basin (Gholampoor et al., 2018). Salmanmahiny et al. (2012) classified LC types of the HRB as rangeland, agriculture, bare land, and saline land with rangeland being the dominant LC type. Notably, saline-tolerant plants are the dominant land cover in the southern parts of the basin. The consequences of salinity in the study area include low agricultural productivity and low economic efficiency of the croplands due to lack of water, as well as soil erosion. In addition, soil in vast area of bare lands (about 4,340 km^2) in the southern parts of the study area is prone to wind erosion generating a source of dust in the surrounding regions notably Garmsar City located in the center. Moreover, because of the escalating trend of desertification in the southern part, the problem has worsened significantly.

2.2 | Data collection and research methods

Generation of a predicted LC map for 2040 involved the following main steps: (a) satellite image preparation, (b) classification of images and extraction of historical LC maps, (c) LC change prediction by

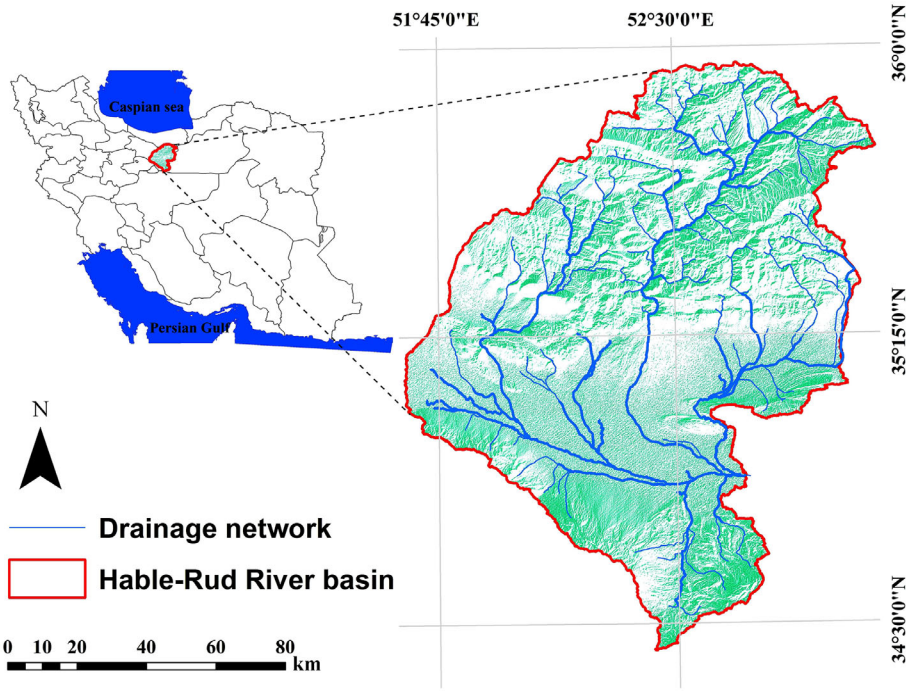

FIGURE 1 Location of the study area in Iran [Colour figure can be viewed at wileyonlinelibrary.com]

TABLE 1 Specifications of LANDSAT images used in this study

Dataset	Date	Source Reference	Band Number
LANDSAT 8 OLI[a] (path/row: 163/35, 163/36, 164/35, and 164/36)	7.18.2017 6.16.2017 6.7.2017 6.7.2017	WGS84	5,4,3,2
LANDSAT 7 ETM+[a] (path/row: 163/35, 163/36, 164/35 and 164/36)	7.28.2000 7.19.2000 7.18.2000 6.25.2000	WGS84	5,4,3,2
LANDSAT 5 TM[a] (path/row: 163/35, 163/36, 164/35 and 164/36)	7.4.1986 7.2.1986 6.11.1986 6.2.1986	WGS84	4,3,2,1

[a]Source: https://earthexplorer.usgs.gov/

applying land change modeler (LCM) and (d) showing the impact of LC changes by interpreting long-term precipitation, streamflow, and sediment load data.

2.3 | Satellite image preparation

For this study, LANDSAT satellite images (level 1) of the Paths/Rows 163/35, 163/36, 164/35, and 164/36 with a resolution of 900 m^2 were accessed through the United States Geological Survey (https://earthexplorer.usgs.gov/). Thus, imageries from the sensors TM, ETM+, and OLI of LANDSATS 5, 7, and 8 were obtained for the years 1986, 2000, and 2017, respectively. The coordinate system used was WGS_1984_UTM_Zone_39N. To reduce the effect of seasonal and phonological changes on the detected land cover changes, the image pairs were selected in the same season or temporally close for all years studied. Land cloud cover (less than 5%) was also a key criterion in selecting images. Radiometric and atmospheric corrections were accomplished to satisfy the preprocessing requirement for change detection. The images using iteratively reweighted multivariate alteration detection (IR-MAD) and fast line-of-sight atmospheric analysis of hypercube (FLAASH) methods in ENVI software were radiometrically and atmospherically corrected, respectively. The detail of the data is shown in Table 1.

Difficulties when processing images included the rugged terrain with mountains in the north and downstream desert areas in the

south and the difference in TM and OLI sensors technologies which could potentially lower classification accuracy.

2.4 | Classification of images and extraction of historical LC maps

All the steps for this section were implemented in the ENVI software version 5.1. First, the study area was divided into six main classes including rangeland, bare land, saline land, agricultural land, industrial area, and residential area (see Table 2). Next, a stratified random sampling technique was used for sampling, and based on colour, tone, the reflectance of LANDSAT images, many training samples were collected for these defined classes. Then, the training samples were allocated to similar and surrounding pixels. After that, to classify and extract historical LC maps, the maximum likelihood classification (ML) method was applied. The ML is a pixel-based supervised statistical classification method that works based on the multivariate probability density of classes (Lillesand et al., 2015), in which class signatures are assumed to have normal distributions. Finally, the accuracy of those trained samples is assessed by the kappa index or the percentage of the correspondence between Google Earth images and the extracted features on the LC maps. To do this, ground control points were selected from Google Earth, and then, the kappa index was estimated between the ground control points and their corresponding points on the extracted maps.

2.5 | Land use/cover prediction by applying the land change modeler (LCM)

The LCM is a tool to predict land changes for land planning (Eastman & Toledano, 2018). The LCM was used due to its simplicity, graphical illustration, and availability of different modeling approaches. The LCM utilizes historical maps of LULC to empirically model the association between LC transitions and descriptive variables to map future LULC scenarios (Eastman & Toledano, 2018). The LCM has been used in many studies worldwide as a new generation of models to detect and model LC change in a wide range of applications (Ansari & Golabi, 2019; Gibson et al., 2018; Li & Liu, 2017; Tarawally et al., 2019). Predicting future LC in the LCM includes four main steps: (a) analyzing historical LC changes, (b) creating transition matrix maps, (c) model validation, and (d) predicting future LC map.

TABLE 2 Class delineation based on supervised classification

Class Name	Description
Agriculture land	Includes all farms and gardens
Rangeland	Includes all range lands and forest fields.
Bare land	Includes all land of no economic value
Saline land	Includes all saline land areas
Industrial land	Includes all industrial areas
Residential areas	Includes all residential areas (cities, villages...)

2.5.1 | Analyzing historical LC changes

The changes in LC were analyzed using the extracted historical maps and in the process, classified image of the year 1986 was compared with that of 2000, and this was repeated for classified images of the year 2000 versus 2017, and 1986 versus 2017.

2.5.2 | Creating transition matrix maps

LC transition matrix maps were created to analyze and determine spatial trends in LC changes as well as LC gains and losses. These maps were made based on one or a group of sub-model(s) in the LCM using a multi-layer perceptron (MLP) artificial neural network (ANN). Artificial neural networks (ANN) easily tackle nonlinearity in data and can provide a good mapping between dependent and independent variables (Wang et al., 2013). The MLP is known as the most practical type of ANN (Razavi & Karamouz, 2007; Razavi & Tolson, 2011). Moreover, the sub-models indicate the probability of changing from one LC class to another over the study period. Based on the major changes in the study area, a large number of sub-models were generated. Based on the main changes that occurred in the area, the number of sub-models can be selected. LCM allows choosing the optimal threshold for selecting the optimal number of sub-models where the users can overlook small changes (Eastman & Toledano, 2018). Accordingly, given the size of the study area, we ignored LC changes less than 100 km^2 (less than 1% of the study area). To choose the best performing LCM, several sub-models were developed using a different combination of those changes and comparing with the historical LC changes. Accordingly, regarding major changes, six sub-models of LC inter-conversion were selected including: (a) bare land conversion to rangeland; (b) rangeland conversion to agricultural land; (c) bare land conversion to saline land; (d) rangeland conversion to saline land; (e) rangeland conversion to bare land; and (f) saline land conversion to bare land.

For each sub-model, descriptive variables were identified as inputs to predict LC maps. Descriptive variables are indicators that influence changes in each class. In the present study, the Cramer's V coefficient was used to select the descriptive variables. This coefficient estimates the strength of association between dependent and independent variables and ranges from zero to one with values close to zero showing a weak association between the variables and those close to one showing a strong association between the variables. This coefficient should be higher than 0.15 for influential variables (Pistocchi et al., 2002). The results of testing the descriptive variables for each LC class are shown in Table 3. The descriptive variables include elevation, slope, aspect (derived from digital elevation model), distance to roads and rivers, and distances to all LC types (agricultural land, saline land, bare land, rangeland, residential area, and industrial area).

TABLE 3 The Cramer's V coefficients for the LC change variables of the HRR

Variables	DEM	Slope	Aspect	Distance to Residential Areas	Distance to Industrial Areas	Distance to Roads	Distance to Rivers	Distance to Bare Lands	Distance to Saline Lands
Overall Cramer's V	0.33	0.24	0.17	0.19	0.17	0.30	0.18	0.32	0.26
Rangeland	0.16	0.12	0.12	0.10	0.14	0.48	0.09	0.17	0.35
Bare land	0.16	0.14	0.23	0.10	0.10	0.23	0.14	0.17	0.23
Saline land	0.23	0.17	0.11	0.19	0.11	0.16	0.17	0.18	0.16
Agriculture	0.12	0.11	0.11	0.13	0.13	0.12	0.05	0.14	0.13
Residential	0.33	0.35	0.27	0.10	0.10	0.26	0.18	0.71	0.23
Industrial	0.15	0.19	0.16	0.19	0.14	0.54	0.14	0.19	0.53

2.5.3 | Model validation

The validation process compares the quality of the predicted map to the extracted map in 2017. There are two different approaches for validation: visual and statistical (Pontius & Malanson, 2005). In this study, the second approach was applied, which considers the agreement between two maps (Pontius & Malanson, 2005). To validate the model, the predicted map of the year 2017 was examined against the extracted map of the same year, via the kappa index which is calculated based on Equation (1) (Cohen, 1960). The kappa Index of agreement indicates the overall accuracy between the two reference maps (extracted and predicted 2017). One of the disadvantages of the standard kappa index is that it ignores the position and quantity of pixels that have been categorized. It examines the chance agreement between the two maps. To obtain a more accurate estimation, the use of the quantity kappa index and location kappa index has been suggested (Pontius & Malanson, 2005). The extracted map (reality) worked as the reference map, while the predicted map was the comparison map.

$$K = \frac{p_a - p_e}{1 - p_e}. \quad (1)$$

Where: $p_a = \frac{1}{n}\sum_{i=1}^{k} nii$. (The relative observed agreement between two maps), and $p_e = \frac{1}{n^2}\sum_{i=1}^{k} n_{i.} n_{.i}$. (The probability of agreement). $K = 1$ has a complete agreement and $K = 0$ has no agreement.

2.5.4 | Predicting future LC map

The extent of LC change expected to occur in the future was predicted by applying the CA algorithm based on the extracted maps of LC types for the past years (1986, 2000, and 2017). CA includes a regular grid of cells that manage how each cell's neighbors affect the future class of each cell (Aviv & Sipper, 1994). CA models typically simulate changes in cells that are near the borders among classes (Benenson & Torrens, 2004). Accordingly, the CA algorithm based on sub-models as the input used to determine the extent of change of one land class to another. The prediction made for LC changes in 2040 was based on multi-objective land allocation (MOLA). The MOLA function used as an extension in the LCM model to allocate the area of each LC type to the predicted map based on the selected sub-models. This function provides a way to resolve multi-objective land allocation problems with conflicting objectives as well as it allow decision-makers to assess the relative priorities of land classes based on a set of preferences, criteria, and indicators for the area. (Hajehforooshnia et al., 2011). It determines a compromise solution that seeks to maximize the suitability of land for each class according to defined sub-models (Geneletti & van Duren, 2008; Hajehforooshnia et al., 2011). Finally, this function identifies the pixels that have the highest probability of converting to specific LC classes in the target year and allocates them to these classes.

2.6 | Land cover changes impact analysis

To assess the possible impacts of the LC changes on hydrological characteristics in the HRB, some meteorological and hydrological variables were analyzed as below.

The precipitation data on a daily basis during the years 1986–2017 from 12 meteorological stations were extracted and analyzed from the Iran Meteorological Organization database. Three meteorological stations from the Meteorological Organization and Iran Ministry of Energy were referred to extract the temperature data. Also, the streamflow and sediment load data for the Bonkouh hydrometric station were extracted and analyzed for the same period from the Iran Ministry of Energy database. The observed data are on a daily and monthly basis for the streamflow and sediment load, respectively. A regression equation between the discharges of streamflow and sediment load was established to estimate sediment load on a monthly basis (Sobhani, 2011). To understand the main cause of streamflow changes, a multiple linear regression was used between streamflow (Y), precipitation (X_1), and temperature (X_2). Consequently, the obtained residual values were analyzed by applying a Mann-Kendall trend test (Helsel & Hirsch, 2002).

3 | RESULTS

3.1 | LC extraction for the past

LC classification results with the ML method for years 1986, 2000, and 2017 are shown in Figure 2. In this study, 142 polygons for LANDSAT TM, 139 polygons for LANDSAT ETM+, and 154 polygons for LANDSAT OLI were selected to evaluate the accuracy of

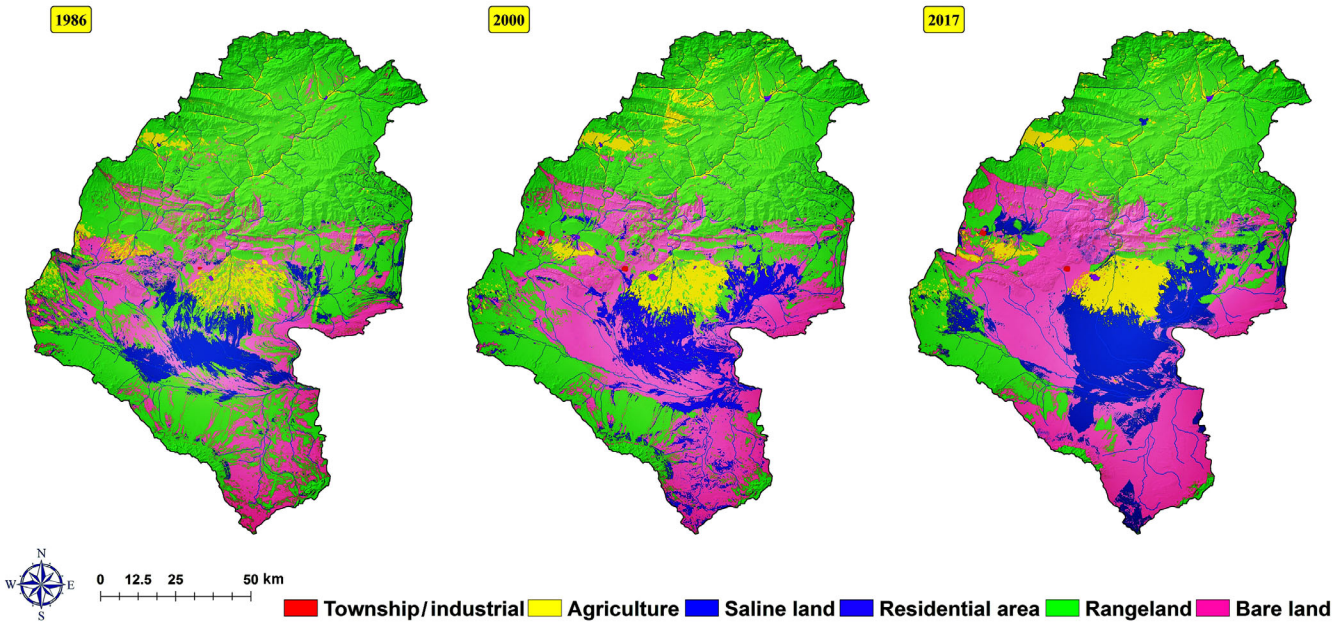

FIGURE 2 The classified LC maps extracted from ENVI 5.1 in 1986, 2000, and 2017 for HRB [Colour figure can be viewed at wileyonlinelibrary.com]

TABLE 4 Classification accuracy (in percent) for different land cover classes

Year	Rangeland	Bare Land	Saline Land	Agricultural Land	Industrial Land	Residential Areas	kappa Index
1986	81.33	79.12	87.23	65.30	68.71	73.42	0.756
2000	79.42	87.28	75.15	83.87	76.18	69.75	0.788
2017	68.72	83.39	81.43	94.31	76.16	63.86	0.811

classification. The assessment results for the three periods are shown in Table 4. The overall classification accuracy values for 1986, 2000, and 2017 were 84.13, 87.14, and 93.78%, respectively. In addition, the kappa index values for the three periods were calculated as 0.756, 0.788, and 0.811, respectively.

The area and percent of LC differences for 1986, 2000, and 2017 are shown in Figure 3. It shows that rangeland was the dominant land cover type in the HRB with an estimated area of 7,904, 6,715, and 5,581 km^2, respectively. Corresponding areas for bare land were 3,249, 3,808, and 4,344 km^2 and those for saline land were 954, 1,319, and 1,823 km^2, respectively. From these land area values, it is evident that from 1986 to 2017 rangeland area was decreased approximately up to about 2,320 km^2; while areas of bare land and saline land were increased by 1,095 and 869 km^2, respectively. Simultaneously, as shown in Figure 3, areas of agricultural land, residential area, and industrial land were also increased. Therefore, during the past 32 years, the area change proportion after rangeland belongs to bare land followed by saline land, agriculture, residential area, and industrial area.

3.2 | LC conversion

We used three different transition matrices for the periods: 1986–2000, 2000–2017, and 1986–2017 and the highest LC conversion between the years 1986 and 2000 was related to rangeland, the area of which decreased by 1,193 km^2 (15%). In contrast, increases were observed for agricultural land [252 km^2 (46%)], saline land [367 km^2 (38%)], bare land [561 km^2 (17%)], industrial land [5.74 km^2 (3%)], and residential area [7.57 km^2 (3%)]. The total area of land conversion for all land classes from 1986 to 2000 was 3,513 km^2 with most of the change related to rangeland (1,903 km^2). In other words, the reduction in the rangeland area was essentially equal to the increase in all other land class areas.

From 2000 to 2017, the LC class with the greatest difference between gains (15%) and losses (42%) was saline land, which experienced a 347 km^2 decrease (26%). Fifteen percent of bare land was converted into other LC classes whereas the conversion into bare land was 29%, resulting in an increase in bare land area of 483 km^2 (13%). This increase in the area of the bare land is most likely resulted from rangeland losses due to a shortage of rainfall during 2000 to 2017 period. The total conversion of one LC class to another from 2000 to 2017 was 2,983 km^2 and most of the changes were related to rangeland (1,844 km^2). The total land conversion in 2000–2017 was 15%, less than that of the period 1986 to 2000. These results are briefly presented in Figure 4.

From 1986 to 2017, the area of rangeland experienced the greatest inter-conversion with other land classes that resulted in 40% gains and 53% losses for a net loss of 13%. Corresponding values for

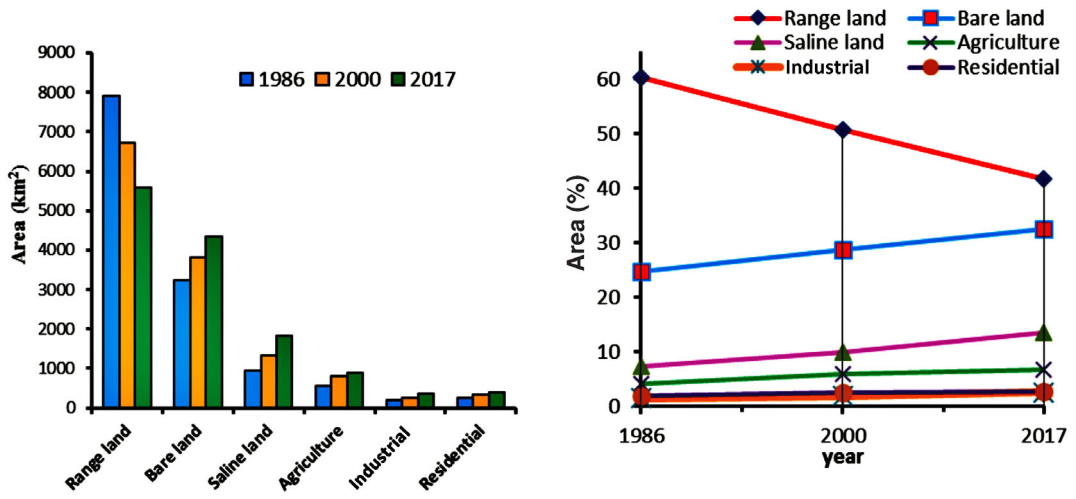

FIGURE 3 Changes in LC area and percent of LC changes in 1986, 2000, and 2017 for the HRB [Colour figure can be viewed at wileyonlinelibrary.com]

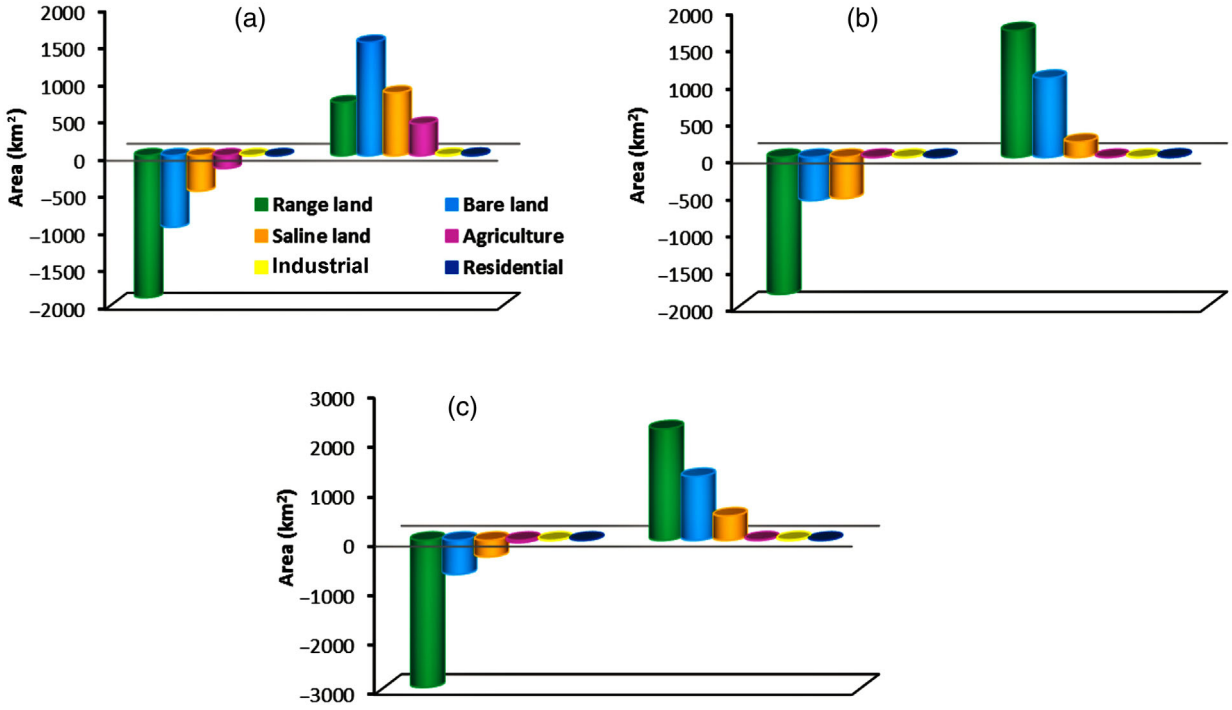

FIGURE 4 Comparison of LC gains and losses from (a) 1986 to 2000, (b) 2000 to 2017, and (c) 1986 to 2017 for HRB [Colour figure can be viewed at wileyonlinelibrary.com]

bare land were 29 and 15%, respectively, for a net gain of 14%, and those for saline land were 26 and 18%, respectively, with a net gain of 8%. The area of agricultural land experienced very little inter-conversion with other land classes and showed a net loss of 4%. No significant inter-conversion occurred with either the residential area or industrial area. Generally, the area of rangeland from 1986 to 2017 decreased by 2,323 km^2 while bare land, saline land, agricultural land, industrial land, and residential area increased by 1,095, 869, 345, 150, and 130 km^2, respectively. The maximum and minimum inter-conversions occurred during the years 1986 to 2017 and 2000 to 2017, respectively.

3.3 | Transition area matrices

The descriptive variables showed in Table 3 were considered as the most important drivers of LC changes in HRB. Regarding the output of MLP, six sub-models were selected including: (a) rangeland to bare

land; (b) rangeland to saline land; (c) rangeland to agricultural land; (d) bare land to rangeland; (e) bare land to saline land; and (f) saline land to bare land. The highest (86.20%) and lowest (49.86%) accuracies were related to the sub-models saline land to bare land and rangeland to agricultural land, respectively.

After creating each sub-model, we studied observed LC for a long period (1986–2017), and then this period was divided into three intervals including 1986–2000, 2000–2017, and 1986–2017 as periods for calibration. Based on the value of the kappa index for each interval, the best one was selected (here 1986–2017). Since the selected interval is prolonged for 32 years, it helps us to justify a feasible future prediction considering some environmental and social variables as descriptive ones. As a result, based on the probability of future changes the spatial distribution pattern of LC for 2040 is modeled and predicted. In the current study, the values for the standard kappa index, quantity kappa index, and location kappa index were 74, 83, and 79%, respectively.

The state transition probability matrices were created from the LC maps for the years 1986 and 2017. Then, the LC map predicted for 2017 and compared to the extracted map of the year 2017. The overall kappa index was close to 74% indicating a moderate agreement (McHugh, 2012). Thus, the LC could be predicted for 2040 (Figure 5). As seen in Figure 5, the area of rangeland and bare land in 2040 will decrease whereas the area of saline land, agricultural land, industrial land, and residential area will increase compared to the predicted map for the year 2017. Saline land in the LC map of 2040 has increased, especially in the southeast of the basin, whereas the area of rangeland decreased more in the southwest of the basin.

3.4 | Land cover changes impacts

Most LC changes for each class in the past and the future are shown in Figure 6. The figure shows remarkable changes in croplands, rangelands, residential, and industrial areas. These changes are more visible for the year 2017 based on LANDSAT 8 imagery showing a great growth in agriculture, saline land, residential, and industrial areas. Figure 6 also shows the change in area for each land cover class. It should be noted that the expansion of some classes such as agriculture, residential, and industrial areas would subsequently increase water consumption and hence would be responsible for the ecological deterioration of the central and southern parts of the HRB. Approaching the future (2040), the central and southern parts of the basin will face an increase in the saline lands. The consequences of salinity may include low agricultural productivity, low economic efficiency, and soil erosion (Hu & Schmidhalter, 2004; Shrivastava & Kumar, 2015).

To show further consequences of LC changes, the long term observed data of precipitation, temperature, streamflow, and sediment load was analyzed in the basin. As mentioned in Section 2.6, based on the data observed at the gauging stations, the required analysis was conducted. Trend analysis of precipitation, temperature, streamflow, and sediment load show that both the observed precipitation and streamflow have negative trends, while the trend of sediment load and temperature show a slight increase during the period (1986–2017) (Figure 7). The mean annual precipitation during 1986–1997, 1997–2008, and 2009–2017 were approximately 125.5, 127, and 88 mm, respectively. In addition, based on the observed data, the mean annual streamflow, sediment load, and temperature in the year

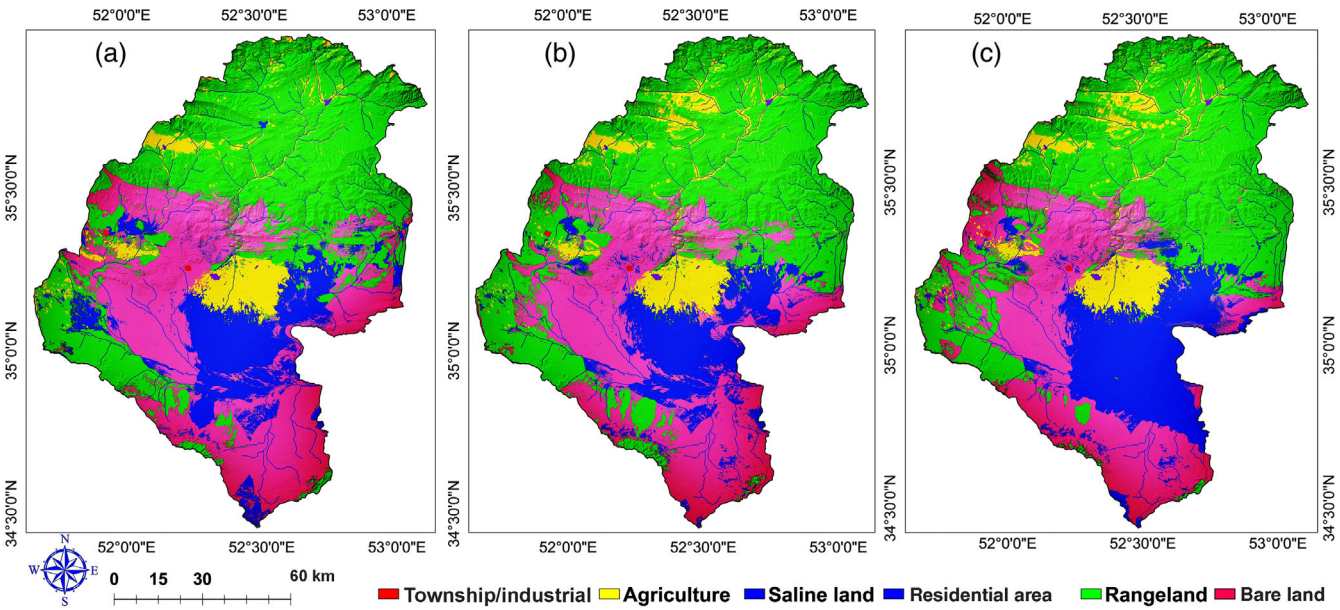

FIGURE 5 The extracted and predicted LC classification: (a) extracted map for 2017, (b) predicted map for 2017, and (c) predicted map for 2040 in the HRB [Colour figure can be viewed at wileyonlinelibrary.com]

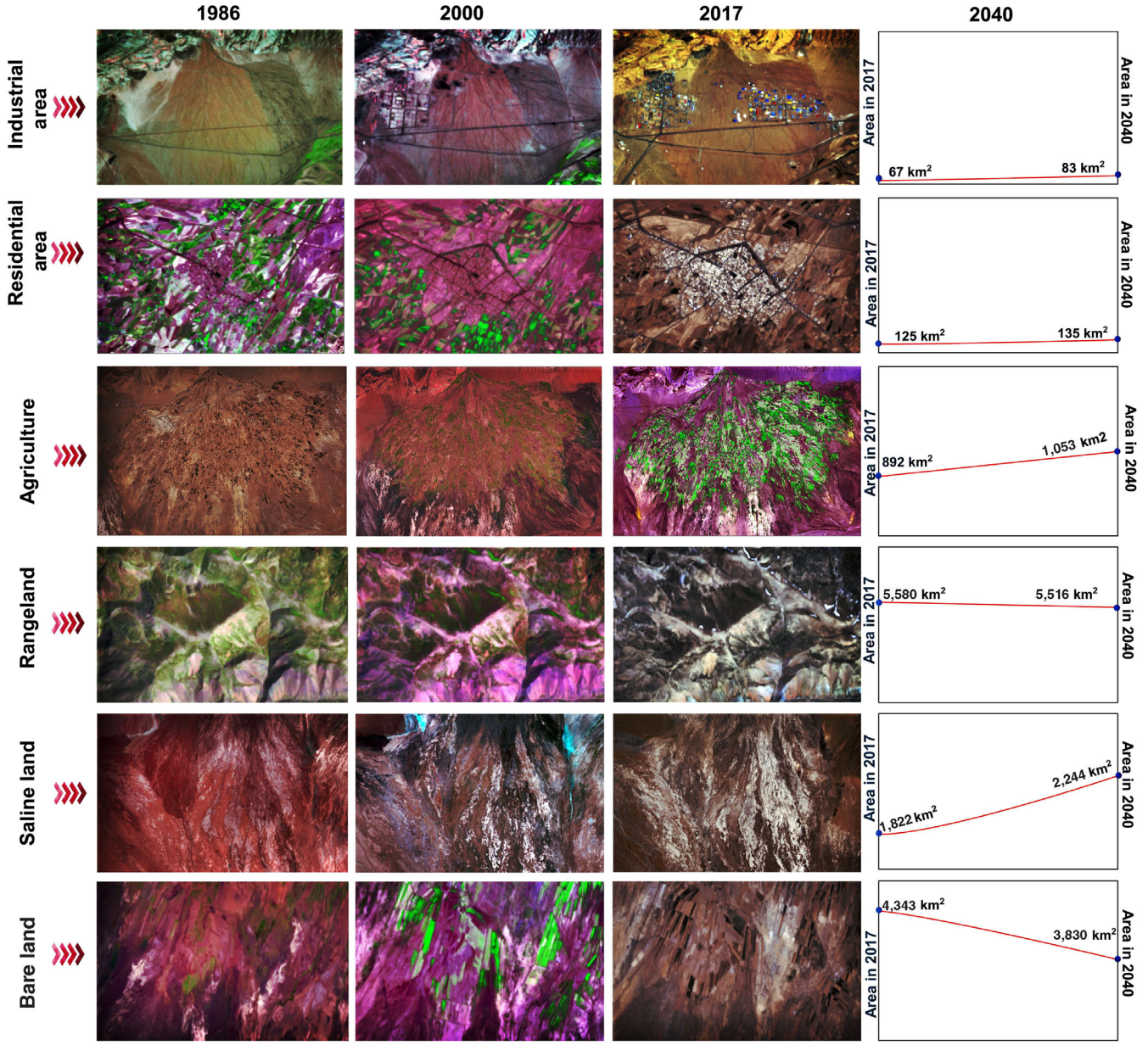

FIGURE 6 Illustration of transitional changes for main land cover classes and the predicted changes in 2040 for the HRB [Colour figure can be viewed at wileyonlinelibrary.com]

intervals were calculated to be approximately 9 $m^3 s^{-1}$, 2.02 million (MTY), and 13.66°C; 5.8 $m^3 s^{-1}$, 2.04 MTY, and 14.37°C; 5.1 $m^3 s^{-1}$, 2.63 MTY, and 15°C, respectively.

The association between streamflow as dependent variable and precipitation and temperature as independent variables was assessed by applying a multiple regression and the obtained residual values were analyzed based on the Mann-Kendall test (Figure 8). Based on Figure 8, since the computed *p*-value is greater than the significance level alpha = 0.05, there is no significant trend in the series, which means that precipitation and temperature are the main responsible factors for the trend detected in the streamflow and after removing these factors no further trend can be identified.

4 | DISCUSSION

This research combined remote sensing (RS) and geographic information systems (GIS) techniques and used the LCM to investigate LC change. The maximum likelihood supervised classification technique was applied to LANDSAT images acquired for 1986, 2000, and 2017. Then, applying a pixel-by-pixel change detection, the LC changes were predicted for 2040 using the LCM. To gain a better accuracy of our prediction, a number of environmental variables used in change modeling include slope, aspect, elevation, and distances to various land features such as rivers, roads, industrial areas, residential areas, saline lands, and agriculture. The outcomes showed that the model

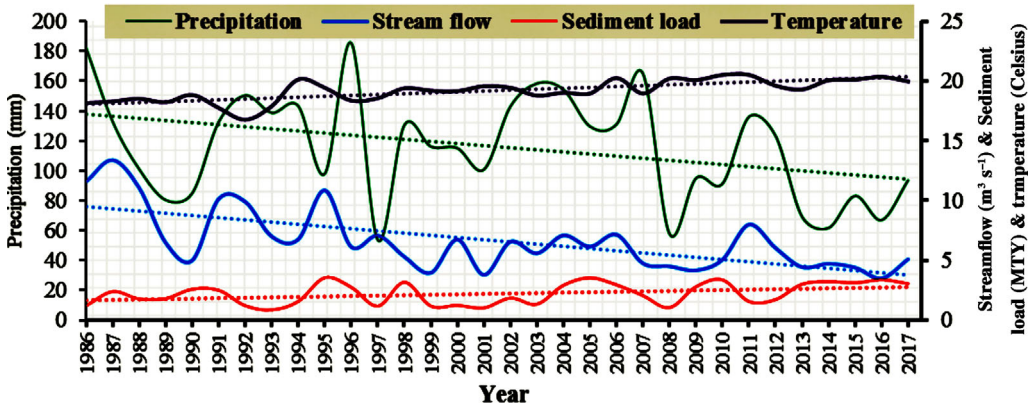

FIGURE 7 Trends of precipitation, temperature, streamflow, and sediment load for the HRB [Colour figure can be viewed at wileyonlinelibrary.com]

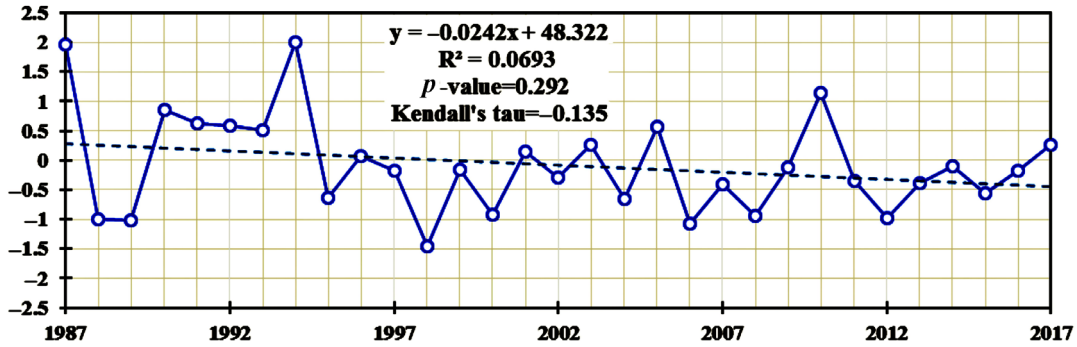

FIGURE 8 Mann-Kendall test of the residual values from a multiple regression of streamflow versus precipitation and temperature during 1986 to 2017 for the HRB [Colour figure can be viewed at wileyonlinelibrary.com]

could predict LC changes in the study area with a kappa index accuracy of 74%. Given the question: "What are the main trends of LC changes in the past and the future of the basin?" the pattern analysis of LC change over the past 32 years shows that the bare land, saline land, agriculture, industrial areas, and residential areas have increased at an average rate of approximately 8, 6.2, 2.7, 0.63, and 0.48%, respectively; while rangeland has decreased by approximately ~18%. The results of the study in applying LANDSAT images to detect land cover changes in arid regions are in a good agreement with Ghare Cheloo et al. (2008), Salmanmahiny et al. (2012), and Alikhah & Froutan (2013). Based on the predicted outcomes for 2040, the areas of agriculture and saline land will increase by approximately ~1.5 and 3%, while the areas of bare land and rangeland will decrease by approximately ~4.55 and 1.45%, respectively. LC change occurs at the local scale, but its ecological impacts spread across regional and global scales (Foley et al., 2005). Most of the lands that are currently under agricultural practice were occupied by forests, rangeland, and wetlands in the past; this conversion has resulted in the loss of biodiversity associated with these natural habitats (Castelletta et al., 2000; Fang et al., 2005).

As shown in Figure 6, there have been some area changes in different land covers in the basin. According to the satellite images of the years 1986, 2000, and 2017, rangeland has undergone significant changes in these periods. Most reduction has taken place during the 1986–2000 period (1,190 km^2) with continuing similar trend over the years 2000 to 2017. Although the rangeland class has decreased over the past 32 years, the agriculture class has increased and it seems to be the main reason for the reduction in rangeland. There are many reasons for this conversion. Firstly, the arid study area has faced several years of drought from 1986 to 2017. Secondly, during this period, rangeland was widely available for conversion to other LC classes. Thus, given the question "What are the major LC changes in the HRB?" it can be concluded that rangeland has been the major LC type that undergone the changes. Development of agriculture (both rainfed and irrigated) started at least two decades ago when the Iranian Government implemented a new strategy for agricultural products (Madani, 2014). The Government raised economic growth with increased agricultural production (Hassanzadeh et al., 2012). More production not only needs more land but also, in this case, more water withdrawal given limited annual precipitation (195 mm). Hence, ensuring food security led to the expansion of the agricultural area mostly at the cost of rangeland (Shirmohammadi et al., 2020). Figure 6 shows that most changes happened between agriculture and rangeland classes. Implementation of development projects without considering the principles of sustainable development, as well as socioeconomic issues, let

stakeholders be unrestricted in changing rangeland to agriculture, particularly over the years 1993–2004 (Alipour & Olya, 2015).

LC plays a significant role in the sustainability of water resources and can have direct and indirect influences inside as well as beyond basin boundaries (Alipour & Olya, 2015; Faramarzi, 2012). The water resources of a river basin primarily depend on input variables such as precipitation (Shirmohammadi et al., 2020). The LC change is considered one of the significant driving forces of alteration in ecosystem factors (Moges & Bhat, 2018). Most of the negative impacts of the LC change is drastic environmental degradation in the form of soil erosion, loss of biodiversity, soil quality deterioration, decreasing availability of water, and saline lands expansion (Miheretu & Yimer, 2017; Wubie et al., 2016). However, the rise in agriculture, residential, and industrial areas will increase water consumption. As shown in Figure 7, streamflow and precipitation trends show that precipitation declined slightly during the period, whereas the observed streamflow presented a striking reduction. Although before 1995 the streamflow and precipitation followed similar trends, but approaching 2017, the precipitation and streamflow represent different trends and behavior. The precipitation declined almost 29%, while the streamflow declined almost 44%. In contrast, the annual temperature and sediment load have increased by 10 and 30% over the same period, respectively (Figure 7). Figure 8 indicates that the LC changes during the past 32 years have not had a significant impact on annual streamflow.

Given the question "What are the environmental consequences of the LC changes in the HRB?" the extracted and predicted LC maps showed a large expansion of saline lands in the basin. Also, trend analysis of sediment load data provides more specific evidence regarding the sensitivity of sediment load to LC changes. This is why sediment load values positively changed although both precipitation and streamflow had a decreasing trend.

This investigation provides an entry point for LC change as part of the discussion on more sustainable and adaptive water management in the basin. Consequently, the outcomes presented in the study should interpreted as an approach to discuss and create awareness of the consequences of LC change.

5 | CONCLUSIONS

This article explores LC classification and change detection and prediction for HRB using the ML algorithm and LCM model in the GIS environment. Various environmental variables were determined and different sub-models were developed to understand the pattern of changes in LC in HRB. The best performing set of the LCM model was developed to predict future changes in LC. Based on the model the future prediction was validated by a standard kappa index of 0.74%. The patterns of LC changes during the 32-year period of 1986–2017 showed that the bare land, saline, agricultural, and industrial lands plus residential areas have increased by approximately 8, 6.2, 2.7, 0.63, and 0.48%, respectively, while rangeland has decreased by approximately 18%. According to the predicted results for the year 2040, agriculture and saline land may increase by approximately 1.5 and 3%, respectively, while the areas of bare land and rangeland land will decrease by approximately 4.55 and 1.45%, respectively. These changes may occur under current scenario that is, considering the chosen sub-models of LC transfers and assuming the existence of the experienced land cover pressures. However, predicting future land cover changes includes various uncertainties which should be taken into account in any application. Uncertainty level depends on many other factors, assumptions, and conditions beyond the scope of this work.

The predicted LC changes suggested by this research could serve as a spatial guideline for monitoring future trends of LC dynamics as well as to address threats brought about by the changes in residential areas and the expansion of agricultural and saline lands. Hence, the rapid growth of residential and agricultural areas and the expansion of saline land in the central and southern parts of the basin have significantly influenced the rangelands and bare lands causing environmental degradation. Evidently, losing rangeland and bare land may bring several negative consequences of which we may cite declining environmental quality, increased water consumption, and greater sediment load.

To conclude, it is vital to formulate and implement some policies and strategies in the basin to prevent or minimize further land cover changes and land degradation. To this end, some relevant tools such as rewarding regulation and legislation, setting penalties, and more importantly education and outreach on the negative impacts of LC changes should be employed by the authorities in the basin. This becomes even more important with the impact of climate change.

ACKNOWLEDGMENTS

We thank the anonymous reviewers for their careful reading of our manuscript and their many insightful comments and suggestions. This research was funded by Gorgan University of Agricultural Sciences and Natural Resources of Iran. Sajad Khoshnoodmotlagh was supported in part by a fellowship from the Integrated Modelling Program for Canada (https://gwf.usask.ca/impc/) at the University of Saskatchewan, Canada.

DATA AVAILABILITY STATEMENT

The data of this study will be available by the corresponding author upon a reasonable request.

ORCID

Amir Sadoddin https://orcid.org/0000-0002-4192-4010

REFERENCES

Aitkenhead, M. J., & Aalders, I. H. (2009). Predicting land cover using GIS, Bayesian and evolutionary algorithm methods. *Journal of Environmental Management*, *90*(1), 236–250. https://doi.org/10.1016/j.jenvman.2007.09.010

Alikhah, M., & Froutan, E. (2013). Use of fuzzy classification method to prepare land use map (a case study of Hable-Rud watershed). *Human and the Environment*, *24*, 42–47.

Alipour, H., & Olya, H. G. T. (2015). Sustainable planning model toward reviving Lake Urmia. *International Journal of Water Resources Development*, *31*(4), 519–539. https://doi.org/10.1080/07900627.2014.949636

Ansari, A., & Golabi, M. H. (2019). Prediction of spatial land use changes based on LCM in a GIS environment for desert wetlands – A case study: Meighan Wetland, Iran. *International Soil and Water Conservation Research*, *7*(1), 64–70. https://doi.org/10.1016/j.iswcr.2018.10.001

Atzberger, C. (2013). Advances in remote sensing of agriculture: Context description, existing operational monitoring systems and major information needs. *Remote Sensing*, *5*(2), 949–981. https://doi.org/10.3390/rs5020949

Aviv, T., & Sipper, M. (1994). Non-uniform cellular automata: Evolution in rule space and formation of complex structures. In R. A. Brooks & P. Maes (Eds.), *Articial Life IV* (pp. 394–399). Cambridge: MIT Press.

Benenson, I., & Torrens, P. M. (2004). Geosimulation: Object-based modeling of urban phenomena. *Computers, Environment and Urban Systems*, *28*(1–2), 1–8. https://doi.org/10.1016/s0198-9715(02)00067-4

Bezak, N., Rusjan, S., Petan, S., Sodnik, J., & Mikoš, M. (2015). Estimation of soil loss by the WATEM/SEDEM model using an automatic parameter estimation procedure. *Environmental Earth Sciences*, *74*(6), 5245–5261. https://doi.org/10.1007/s12665-015-4534-0

Bhat, P. A., Shafiq, M. u., Mir, A. A., & Ahmed, P. (2017). Urban sprawl and its impact on landuse/land cover dynamics of Dehradun City, India. *International Journal of Sustainable Built Environment*, *6*(2), 513–521. https://doi.org/10.1016/j.ijsbe.2017.10.003

Castelletta, M., Sodhi, N. S., & Subaraj, R. (2000). Heavy extinctions of forest avifauna in Singapore: Lessons for biodiversity conservation in Southeast Asia. *Conservation Biology*, *14*(6), 1871–1879. https://doi.org/10.1111/j.1523-1739.2000.99285.x.

Cohen, J. (1960). A coefficient of agreement for nominal scales. *Educational and Psychological Measurement*, *1*, 37–46.

Dewan, A. M., Yamaguchi, Y., & Rahman, M. Z. (2012). Dynamics of land use/cover changes and the analysis of landscape fragmentation in Dhaka Metropolitan, Bangladesh. *GeoJournal*, *77*(3), 315–330. https://doi.org/10.1007/s10708-010-9399-x

Di Gregorio, A., & Jansen, L. J. M. (2000). Land cover classification system (LCCS): Classification concepts and user manual. *FAO*, *53*(May), 179. https://doi.org/10.1017/CBO9781107415324.004

Eastman, J. R., & Toledano, J. (2018). A short presentation of the land change modeler (LCM). *Lcm*, *36*, 499–505. https://doi.org/10.1007/978-3-319-60801-3_36

Etemadi, H., Smoak, J. M., & Karami, J. (2018). Land use change assessment in coastal mangrove forests of Iran utilizing satellite imagery and CA–Markov algorithms to monitor and predict future change. *Environmental Earth Sciences*, *77*(5), 3–13. https://doi.org/10.1007/s12665-018-7392-8

Fang, J., Rao, S., & Zhao, S. (2005). Human-induced long-term changes in the lakes of the Jianghan Plain, Central Yangtze. *Frontiers in Ecology and the Environment*, *3*(4), 186–192. https://doi.org/10.1890/1540-9295(2005)003[0186:HLCITL]2.0.CO;2

Faramarzi, N. (2012). *Agricultural water use in Lake Urmia basin, Iran: An approach toadaptive policies and transition to sustainable irrigation water use*. Ph.D. Thesis, Uppsala University. pp. 43–61. http://hdl.handle.net/20.500.12424/3773174

Farjad, B., Gupta, A., Razavi, S., Faramarzi, M., & Marceau, D. J. (2017). An integrated modelling system to predict hydrological processes under climate and land-use/cover change scenarios. *Water (Switzerland)*, *9*(10), 1–23. https://doi.org/10.3390/w9100767

Feng, K., Siu, Y. L., Guan, D., & Hubacek, K. (2012). Assessing regional virtual water flows and water footprints in the Yellow River basin, China: A consumption based approach. *Applied Geography*, *32*(2), 691–701. https://doi.org/10.1016/j.apgeog.2011.08.004

Fisher, P., Comber, A., & Wadsworth, R. (2005). Land use and land cover: Contradiction or complement. Re-presenting GIS. In *Re-Presenting GIS* (pp. 85–98). United Kingdom: John Wiley and Sons Ltd.

Foley, J. A., DeFries, R., Asner, G. P., Barford, C., Bonan, G., Carpenter, S. R., … Snyder, P. K. (2005). Global consequences of land use. *Science*, *309*(5734), 570–574. https://doi.org/10.1126/science.1111772

Geneletti, D., & van Duren, I. (2008). Protected area zoning for conservation and use: A combination of spatial multicriteria and multiobjective evaluation. *Landscape and Urban Planning*, *85*(2), 97–110. https://doi.org/10.1016/j.landurbplan.2007.10.004

Ghare Cheloo, S., Fayezniya, S., & Mir, K. (2008). Study of Geomorphological formations based on landscape analysis and Satellite Images. *Iranian Journal of Geology*, *8*, 3–16. https://www.sid.ir/fa/journal/ViewPaper.aspx?id=94226.

Gholampoor, A., Ashrafzadeh, A., Piermoradian, N., & Mousavi, A. (2018). Investigating the role of downscaling and the method of calculating reference evapotranspiration in the analysis of the effect of climate change on water resources. *Iranian Soil and Water Research*, *4*(47), 841–852. https://doi.org/10.22059/ijswr.2018.240855.667748

Ghorbani Kalkhajeh, R., & Jamali, A. A. (2019). Analysis and predicting the trend of land use/cover changes using neural network and systematic points statistical analysis (SPSA). *Journal of the Indian Society of Remote Sensing*, *47*(9), 1471–1485. https://doi.org/10.1007/s12524-019-00995-7

Gibson, L., Münch, Z., Palmer, A., & Mantel, S. (2018). Future land cover change scenarios in South African grasslands – Implications of altered biophysical drivers on land management. *Heliyon*, *4*(7), 4–25. https://doi.org/10.1016/j.heliyon.2018.e00693

Groom, G., Mücher, C. A., Ihse, M., & Wrbka, T. (2006). Remote sensing in landscape ecology: Experiences and perspectives in a European context. *Landscape Ecology*, *21*(3 SPEC. ISS., 391–408. https://doi.org/10.1007/s10980-004-4212-1

Gu, Q., Hu, H., Ma, L., Sheng, L., Yang, S., Zhang, X., … Chen, L. (2019). Characterizing the spatial variations of the relationship between land use and surface water quality using self-organizing map approach. *Ecological Indicators*, *102*(March), 633–643. https://doi.org/10.1016/j.ecolind.2019.03.017

Hajehforooshnia, S., Soffianian, A., Mahiny, A. S., & Fakheran, S. (2011). Multi objective land allocation (MOLA) for zoning Ghamishloo Wildlife Sanctuary in Iran. *Journal for Nature Conservation*, *19*(4), 254–262. https://doi.org/10.1016/j.jnc.2011.03.001

Hassanzadeh, E., Zarghami, M., & Hassanzadeh, Y. (2012). Determining the main factors in declining the Urmia Lake level by using system dynamics modeling. *Water Resources Management*, *26*(1), 129–145. https://doi.org/10.1007/s11269-011-9909-8

Helsel, D. R., & Hirsch, R. M. (2002). Techniques of water-resources investigations of the United States Geological Survey book 4. In *Hydrologic analysis and interpretation statistical methods in water resources*. Reston, VA: US Geological Survey. http://water.usgs.gov/pubs/twri/twri4a3/

Hu, Y., & Schmidhalter, U. (2004). *Limitation of salt stress to plant growth*. (4th ed.), pp. 191–224. https://doi.org/10.1201/9780203023884.ch5

IPCC. (2000). *Special report on emissions scenarios. Working Group III, Intergovernmental Panel on Climate Change (IPCC)* (p. 595). Cambridge: Cambridge University Press.

Islam, K., Rahman, M. F., & Jashimuddin, M. (2018). Modeling land use change using cellular automata and artificial neural network: The case of Chunati Wildlife Sanctuary, Bangladesh. *Ecological Indicators*, *88* (February), 439–453. https://doi.org/10.1016/j.ecolind.2018.01.047

Lambin, E. F. (1997). Modelling and monitoring land-cover change processes in tropical regions. *Progress in Physical Geography*, *21*, 375–393. https://doi.org/10.1177/030913339702100303

Li, J., & Liu, C.-m. (2017). Improvement of LCM model and determination of model parameters at watershed scale for flood events in Hongde

basin of China. *Water Science and Engineering*, *10*(1), 36–42. https://doi.org/10.1016/j.wse.2017.03.006

Lillesand, T., Kiefer, R. W., & Chipman, J. (2015). *Remote sensing and image interpretation* (Vol. 7). Washington: Wiley.

Lu, D., Mausel, P., Brondízio, E., & Moran, E. (2004). Change detection techniques. *International Journal of Remote Sensing*, *25*(12), 2365–2407. https://doi.org/10.1080/0143116031000139863

Madani, K. (2014). Water management in Iran: What is causing the looming crisis? *Journal of Environmental Studies and Sciences*, *4*(4), 315–328. https://doi.org/10.1007/s13412-014-0182-z

Magesh, N. S., & Chandrasekar, N. (2017). Driving forces behind land transformations in the Tamiraparani sub-basin, South India. *Remote Sensing Applications: Society and Environment*, *8*(July), 12–19. https://doi.org/10.1016/j.rsase.2017.07.003

Mahiny, A. S., & Clarke, K. C. (2012). Guiding SLEUTH land-use/land-cover change modeling using multicriteria evaluation: Towards dynamic sustainable land-use planning. *Environment and Planning B: Planning and Design*, *39*(5), 925–944. https://doi.org/10.1068/b37092

Marceau, D. J., Wang, F., & Wijesekara, N. (2013). Investigating land-use dynamics at the periphery of a fast-growing city with cellular automata at two spatial scales. *Modeling of Land-Use and Ecological Dynamics*, *November*, *2013*, 51–79. https://doi.org/10.1007/978-3-642-40199-2

McHugh, M. L. (2012). Lessons in biostatistics interrater reliability: The kappa statistic. *Biochemica Medica*, *22*(3), 276–282. https://hrcak.srce.hr/89395

Miheretu, B. A., & Yimer, A. A. (2017). Determinants of farmers' adoption of land management practices in Gelana sub-watershed of northern highlands of Ethiopia. *Ecological Processes*, *6*(1), 2–11. https://doi.org/10.1186/s13717-017-0085-5

Moges, D. M., & Bhat, H. G. (2018). An insight into land use and land cover changes and their impacts in the Rib watershed, Northwestern Highlands, Ethiopia. *Land Degradation & Development*, *29*(10), 3317–3330. https://doi.org/10.1002/ldr.3091

Moss, M. R. (1987). Landscape ecology and management. *First symposium of the Canadian society for landscape ecology and management* (Vol. *2*). https://doi.org/10.1007/978-4-431-54871-3

Ozturk, D. (2015). Urban growth simulation of Atakum (Samsun, Turkey) using cellular automata-Markov chain and multi-layer perceptron-Markov chain models. *Remote Sensing*, *7*(5), 5918–5950. https://doi.org/10.3390/rs70505918

Paegelow, M., & Camacho Olmedo, M. T. (2005). Possibilities and limits of prospective GIS land cover modelling - A compared case study: Garrotxes (France) and Alta Alpujarra, Granada (Spain). *International Journal of Geographical Information Science*, *19*(6), 697–722. https://doi.org/10.1080/13658810500076443

Peraza-Castro, M., Ruiz-Romera, E., Meaurio, M., Sauvage, S., & Sánchez-Pérez, J. M. (2018). Modelling the impact of climate and land cover change on hydrology and water quality in a forest watershed in the Basque Country (Northern Spain). *Ecological Engineering*, *122* (February), 315–326. https://doi.org/10.1016/j.ecoleng.2018.07.016

Pistocchi, A., Luzi, L., & Napolitano, P. (2002). The use of predictive modeling techniques for optimal exploitation of spatial databases: A case study in landslide hazard mapping with expert system-like methods. *Environmental Geology*, *41*(7), 765–775. https://doi.org/10.1007/s002540100440

Pontius, G. R., & Malanson, J. (2005). Comparison of the structure and accuracy of two land change models. *International Journal of Geographical Information Science*, *19*(2), 243–265. https://doi.org/10.1080/13658810410001713434

Ralha, C. G., Abreu, C. G., Coelho, C. G. C., Zaghetto, A., Macchiavello, B., & Machado, R. B. (2013). A multi-agent model system for land-use change simulation. *Environmental Modelling and Software*, *42*, 30–46. https://doi.org/10.1016/j.envsoft.2012.12.003

Razavi, S., & Karamouz, M. (2007). Adaptive neural networks for flood routing in river systems. *Water International*, *32*(3), 360–375. https://doi.org/10.1080/02508060708692216

Razavi, S., & Tolson, B. A. (2011). A new formulation for feedforward neural networks. *IEEE Transactions on Neural Networks*, *22*(10), 1588–1598. https://doi.org/10.1109/TNN.2011.2163169

Salmanmahiny, A., Jazi, H., Karimipour, H., Mehri, A., Kamyiab, H., Zare, A., Mansouri, M., & (2012). Assessing the potential and landscaping of integrated watershed management. In *Land assessment and planning for integrated management of Hable-Rud watershed* (Vol. 1, pp. 1–336). Tehran, Iran: Poune Pub.

Sangermano, F., Toledano, J., & Eastman, R. (2012). Land cover change in the Bolivian Amazon and its implications for REDD+ and endemic biodiversity. *Landscape Ecology*, *27*(4), 571–584. https://doi.org/10.1007/s10980-012-9710-y

Shirmohammadi, B., Malekian, A., Salajegheh, A., Taheri, B., Azarnivand, H., Malek, Z., & Verburg, P. H. (2020). Scenario analysis for integrated water resources management under future land use change in the Urmia Lake region, Iran. *Land Use Policy*, *90*, 30–43. https://doi.org/10.1016/j.landusepol.2019.104299

Shrivastava, P., & Kumar, R. (2015). Soil salinity: A serious environmental issue and plant growth promoting bacteria as one of the tools for its alleviation. *Saudi Journal of Biological Sciences*, *22*(2), 123–131. https://doi.org/10.1016/j.sjbs.2014.12.001

Singh, S. K., Mustak, S., Srivastava, P. K., Szabó, S., & Islam, T. (2015). Predicting spatial and Decadal LULC changes through cellular automata Markov chain models using earth observation datasets and geo-information. *Environmental Processes*, *2*(1), 61–78. https://doi.org/10.1007/s40710-015-0062-x

Sobhani, H. (2011). *Investigating the effect of data classification models on the accuracyof sediment load estimates in the Hable-Rud basin*.M.SC. Thesis. Tehran University. www.hablehroud.ir

Stefanov, W. L., Ramsey, M. S., & Christensen, P. R. (2002). Monitoring urban land cover change. *Remote Sensing of Environment*, *77*(2), 173–185. https://doi.org/10.1016/s0034-4257(01)00204-8

Subedi, P., Subedi, K., & Thapa, B. (2013). Application of a hybrid cellular automaton – Markov (ca-markov) model in land-use change prediction: A case study of Saddle Creek drainage basin, Florida. *Applied Ecology and Environmental Sciences*, *1*(6), 126–132. https://doi.org/10.12691/aees-1-6-5

Tarawally, M., Wenbo, X., Weiming, H., Mushore, T. D., & Kursah, M. B. (2019). Land use/land cover change evaluation using land change modeller: A comparative analysis between two main cities in Sierra Leone. *Remote Sensing Applications: Society and Environment*, *16* (February), 100262. https://doi.org/10.1016/j.rsase.2019.100262

Turner, B. R. H. Moss, D. L. S. (1993). Relating land-use and global land-cover changes. *IGBP report*. Vol. No. 24. https://asu.pure.elsevier.com/en/publications/relating-land-use-and-global-land-cover-change-2

Ulbricht, K. A., & Heckendorff, W. D. (1998). Satellite images for recognition of landscape and landuse changes. *ISPRS Journal of Photogrammetry and Remote Sensing*, *53*(4), 235–243. https://doi.org/10.1016/S0924-2716(98)00006-9

Usharani, K., & Lakshmanaperumalsamy, P. (2011). Bio-treatment of phosphate from synthetic wastewater using pseudomonas sp YLW-7. *Journal of Applied Sciences and Environmental Management*, *14*(2), 75–80. https://doi.org/10.4314/jasem.v14i2.57867

Verburg, P. H., Neumann, K., & Nol, L. (2011). Challenges in using land use and land cover data for global change studies. *Global Change Biology*, *17*(2), 974–989. https://doi.org/10.1111/j.1365-2486.2010.02307.x

Wang, H., Shen, Q., Tang, B. S., & Skitmore, M. (2013). An integrated approach to supporting land-use decisions in site redevelopment for urban renewal in Hong Kong. *Habitat International*, *38*(1), 70–80. https://doi.org/10.1016/j.habitatint.2012.09.006

Wubie, M. A., Assen, M., & Nicolau, M. D. (2016). Patterns, causes and consequences of land use/cover dynamics in the Gumara watershed

of Lake Tana basin, Northwestern Ethiopia. *Environmental Systems Research*, *5*(1), 1–12. https://doi.org/10.1186/s40068-016-0058-1

Yang, X., Zheng, X. Q., & Lv, L. N. (2012). A spatiotemporal model of land use change based on ant colony optimization, Markov chain and cellular automata. *Ecological Modelling*, *233*, 11–19. https://doi.org/10.1016/j.ecolmodel.2012.03.011

Zheng, H. W., Shen, G. Q., Wang, H., & Hong, J. (2015). Simulating land use change in urban renewal areas: A case study in Hong Kong. *Habitat International*, *46*, 23–34. https://doi.org/10.1016/j.habitatint.2014.10.008

How to cite this article: Khoshnood Motlagh, S., Sadoddin, A., Haghnegahdar, A., Razavi, S., Salmanmahiny, A., & Ghorbani, K. (2021). Analysis and prediction of land cover changes using the land change modeler (LCM) in a semiarid river basin, Iran. *Land Degradation & Development*, 1–14. https://doi.org/10.1002/ldr.3969